JOC Article

Internally Solvated Cyclopentadienyllithium Compounds: Structural Integrity of the Cp^-Li^+ Moiety. NMR, Dynamics, X-ray Crystallography, and Calculations

Gideon Fraenkel,* Xiao Chen, Albert Chow, Judith C. Gallucci, and Hua Liu

Department of Chemistry, Ohio State University, Columbus, Ohio 43210

fraenkel@mps.ohio-state.edu

Received June 17, 2005

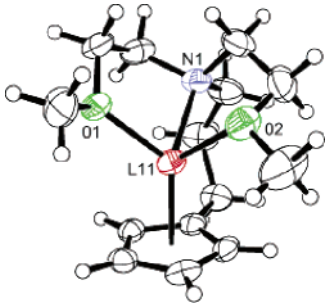

Three cyclopentadienyllithium compounds with the tethered, T, ligand $-N(CH_2CH_2OCH_3)_2$ are as follows: T = $CHCH(CH_3)_2$, **6**; T = $(CH_2)_2$, **10**; T = $(CH_2)_3$, **14**. The results of NOE NMR experiments for **6**, **10**, and **14** together with X-ray crystallography of **14** support internally coordinated monomeric structures for all three compounds. Models have been constructed for **6**, **10**, and **14** from modifications of an internally solvated allylic lithium compound at the B3LYP level of theory using basis set 6-311G*. The resulting structural features are very similar to those obtained from the NMR and crystallographic data. In addition, ^{13}C NMR shifts obtained with the GIAO procedure using the results of the B3LYP/6-311G* calculations are closely similar to the experimental shifts, which validate B3LYP as a suitable model for these compounds. The Li^+ centroid distance of ca. 1.9 Å to 2.0 Å obtained for **6**, **10**, and **14** is common to most crystallographic data for externally solvated Cp^-Li^+ compounds as well as one which incorporates a $(CpLiCp)^-$ triple ion. It is concluded that the ligand tether and the stereochemistry around Li^+ accommodate to maintain the structural integrity of Cp^-Li^+. NMR and crystallography show **14** to be chiral. Carbon-13 NMR line shape changes are attributed to inversion via a lateral wobble mechanism with $\Delta H^{\ddagger} = 6$ kcal·mol^{-1} and $\Delta S^{\ddagger} = -2$ eu. It is also shown that a 6,6-dimethylfulvene is deprotonated at methyl by $LiN(CH_2CH_2OCH_3)_3$ as well as by butyllithium in the presence of PMDTA producing isopropenyl Cp^-Li^+ compounds **24** and **25**, respectively. NMR line shape changes of the sample containing **24** have been qualitatively interpreted to result from a combination of fast transfer of coordinated ligand between faces of the carbanion plane as well as a lithium-exchange process.

Introduction

Among the results of X-ray crystallographic,[1] NMR,[2] and calculational studies[3] of organolithium compounds it is commonly found that allylic lithium compounds incorporate delocalized carbanions within contact ion-paired species.[1a−i,2c−h,3a−g] For example, in externally solvated allyllithium, coordinated Li^+ is sited normal to the center of the delocalized allyl plane; see **1**.[4]

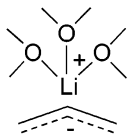

1

In experiments to slow intermolecular exchange processes among ion pairs and thus facilitate NOE studies of their structure, several internally coordinated allylic[5] and benzylic[6] lithium compounds were prepared. It was anticipated that encapsulating the lithium by internal coordination to a pendant ligand would severely reduce the rates of intermolecular exchange of ions between ion pairs. However, several of the resulting compounds did

10.1021/jo0512507 CCC: $30.25
Published on Web 10/11/2005

not incorporate delocalized carbanions. For example, deprotonation of **2** with CH_3Li in diethyl ether or THF produced a compound best described as **3** on the basis of X-ray crystallographic and NMR studies.[5a,b,7] It was

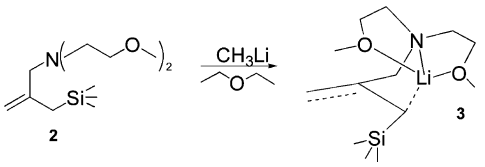

proposed that the ligand tether is too short to place Li^+ normal to the center of the allyl plane as in **1**. Instead, Li^+ is sited above the allyl plane near the C−Si allyl terminal.[7] The Li^+ so placed polarizes the allyl moiety to become partially localized.[7] Several related compounds showed similar effects.[7] This established a principle that the degree of conjugation of an ordinarily delocalized carbanion depends on the site of the counterion with respect to the anion. In the study reported herein, we have investigated the possible operation of such effects among internally coordinated cyclopentadienyllithium compounds. Changing the length of the ligand tether should in principle change the position of Li^+ relative to the carbons in the Cp^- ring and thus perturb the Cp^- structure to different degrees.

TABLE 1. ^{13}C and (^1H) Chemical Shifts, δ Scale, Internally Solvated Cp^-Li^+ Compounds 6, 10, and 14

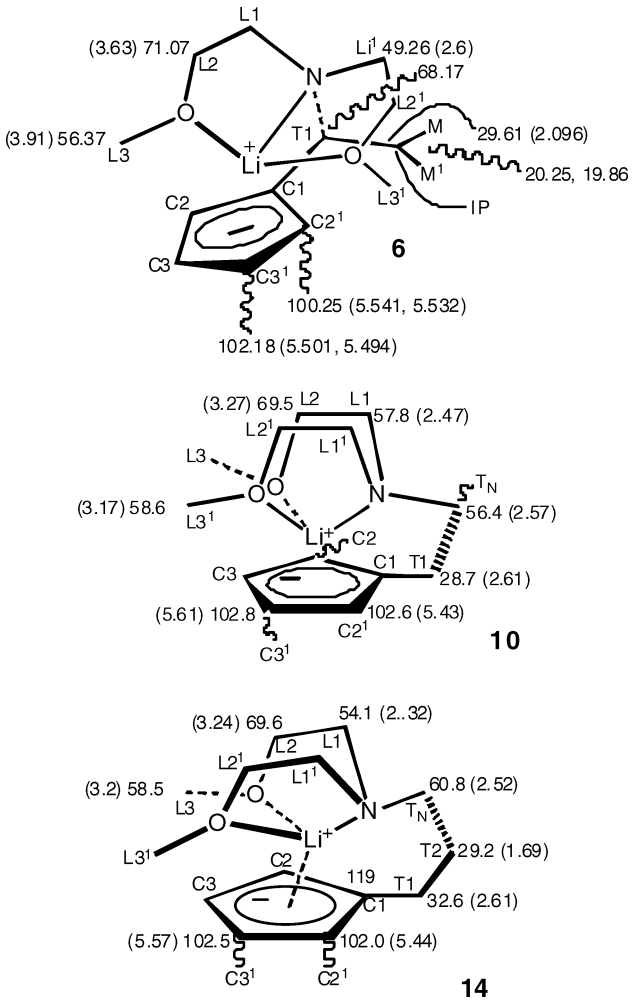

Results and Discussion

Reactions 1−5 involving starting materials and intermediates **4**, **5**, **7**−**9**, and **11**−**13** summarize the preparation of three internally solvated cyclopentadienyllithium compounds **6**, **10**, and **14**. Needless to say, the isomeric dienes **8** and **9** were prepared and used as mixtures as is also the case for the pair **12** and **16**. For convenience, the ^{13}C and ^1H NMR chemical shifts are listed around the structures of **6**, **10**, and **14** in Table 1.

The simplest approach to preparing a cyclopentadientyllithium with a one-carbon tethered ligand **6** is to add the appropriate organometallic or lithium amide to a fulvene,[8] see (1). A substituted fulvene was used since

(1) (a) Weiss, E. *Angew. Chem., Int. Ed. Engl.* **1993**, *32*, 1501−1570. (b) Williard, P. G. Carbanions of Alkali and Alkaline Earth Cations: (1) "Synthesis and Structural Characterization. In *Comprehensive Organic Synthesis, Selectivity and Strategy and Efficiency in Organic Chemistry*; Trost, B. M., Fleming, I., Eds.; Pergamon Press: Oxford, 1991; pp 1−48. (c) Boche, G. *Angew. Chem., Int. Ed. Engl.* **1989**, *28*, 277−297. (d) Den'yanov, P.; Boche, G.; Marsch, M.; Harms, K.; Fyodorova, G.; Petroysan, V. *Liebigs Ann. Chem.* **1995**, 457. (e) Boche, G.; Fraenkel, G.; Cabral, J.; Harms, K.; van E. Hommes, N. J. R.; Johrenz, J.; Marsch, M.; Schleyer, P. v. R. *J. Am. Chem. Soc.* **1992**, *114*, 1562. (f) Marsch, M.; Harms, K.; Zschage, G.; Hopper, D.; Boche, G. *Angew Chem., Int. Ed. Engl.* **1991**, *30*, 321. (g) Hitchcock, P. S.; Lappert, M. F.; Wang, Zhong-Xia. *J. Chem. Soc., Chem. Commun.* **1996**, 1647. (h) Seebach, D.; Maetzke, T.; Haynes, R. K.; Paddon-Row, M. N. *Helv. Chim. Acta* **1988**, *71*, 299. (i) Cragg-Hine, I.; Davidson, M. G.; Mair, P. S.; Snaith, R. *J. Chem. Soc., Dalton. Trans.* **1993**, 2423.

(2) Reviewed (a) Günther, H. Lithium NMR. In *Encyclopedia of NMR*; Becker, E., Ed.; J. Wiley and Sons: New York, 1996; Vol. 5, pp 2807−2828. (b) Bauer, W.; Schleyer, P. v. R. Recent Results in NMR Spectroscopy of Organolithium Compounds. In *Advances in Carbnion Chemistry*; Sniekus, V., Ed.; JAI Press: Greenwich, CT, 1992; Vol. 1, pp 81−175. (c) West, P.; Purmort, J. I.; McKinley, S. V. *J. Am. Chem. Soc.* **1968**, *90*, 797. (d) Bates, R. D.; Beavers, W. *J. Am. Chem. Soc.* **1974**, *96*, 5001. (e) Thompson, T. B.; Ford, W. T. *J. Am. Chem. Soc.* **1974**, *101*, 5459. (f) Benn, R.; Rufinska, A. *J. Organomet. Chem.* **1982**, *239*, C19. (g) Fraenkel, G.; Chow, A.; Winchester, W. R. *J. Am. Chem. Soc.* **1990**, *112*, 1382−1386. (h) Fraenkel, G.; Cabral, J.; Lanter, C.; Wang, J. *J. Org. Chem.* **1999**, *64*, 1302−1310. (i) Fox, T.; Hansmana, H.; Günther, H. *Magn. Reson. Chem.* **2004**, *42*, 788−794. (j) Pepels, A.; Günther, H.; Ainoureux, J.-P.; Fernendaz, C. *J. Am. Chem. Soc.* **2000**, *122*, 9858. (k) Ramirez, A.; Lobkovsky, E.; Collum, D. B. *J. Am. Chem. Soc.* **2003**, *125*, 15376−15387. (l) Briggs, T. F.; Winemuller, M. D.; Xiang, B.; Collum, D. B. *J. Org. Chem.* **2001**, *66*, 6291−6298. (m) Sun, X.; Winemuller, M. D.; Xiang, B.; Collum, D. B. *J. Am. Chem. Soc.* **2001**, *123*, 8039−8046. (n) Reich, H. J.; Goldenberg, W. S.; Sanders, A. W.; Jantzi, K. L.; Tzschucke, C. C. *J. Am. Chem. Soc.* **2003**, *125*, 3509. (o) Reich, H. J.; Goldenberg, W. S.; Gudmundsson, B. O.; Sanders, A. W.; Kulicke, K. J.; Sinou, K.; Guzer, I. A. *J. Am. Chem. Soc.* **2001**, *123*, 8067−8079. (p) Reich, H. J.; Goldenberg, W. S.; Sanders, A. W.; Tzschucke, C. C. *Org. Lett.* **2001**, 33−36.

(3) (a) Eusalimski, C. B.; Kormer, V. H. *Zh. Org. Khim.* **1984**, *20*, 208. (b) Tidwell, E. R.; Russell, E. R. *J. Organomet. Chem.* **1983**, *259*, 81. (c) Clarke, T.; Jemmis, E. D.; Schleyer, P. v. R.; Binkley, J. S.; Pople, J. A. *J. Orgnometal. Chem.* **1978**, *150*, 1. (d) Clarke, T.; Rhode, C.; Schleyer, P. v. R. *Organometallics* **1983**, *2*, 1344. (e) Bushby, R. J.; Tytho, M. P. *J. Organomet. Chem.* **1984**, *270*, 205. (f) Pratt, L. M.; Khan, I. M. *J. Comput. Chem.* **1995**, *16*, 1070. (g) Eikemma-Hommes, N. J. R. Van; Bühl, M.; Schleyer, P. v. R. *J. Organomet. Chem.* **1991**, *409*, 307−320. (h) Sapse, A.-M.; Jain, D. C.; Raghavachari, K. Theoretical Studies of Aggregates of Lithium Compounds. In *Lithium Chemistry, A Theoretical and Experimental Overview*; Sapse, A.-M., Schleyer, P. v. R., Eds.; Wiley-Interscience: New York, 1995; pp 45−67.

(4) Schumman, U.; Weiss, E.; Dietrich, H.; Mahdi, W. *J. Organomet. Chem.* **1987**, *322*, 299.

(5) (a) Fraenkel, G.; Qiu, F. *J. Am. Chem. Soc.* **1996**, *118*, 5828. (b) Fraenkel, G.; Qiu, F. *J. Am. Chem. Soc.* **1997**, *119*, 3571−3577. (c) Fraenkel, G.; Duncan, J. H.; Wang, J. *J. Am. Chem. Soc.* **1999**, *121*, 432−443.

(6) (a) Fraenkel, G.; Martin, K. *J. Am. Chem. Soc.* **1995**, *117*, 10336−10344. (b) Fraenkel, G.; Duncan, J. H.; Martin, K. *J. Am. Chem. Soc.* **1999**, *121*, 10538−10544.

(7) Fraenkel, G.; Chow, A.; Fleischer, R.; Liu, H. *J. Am. Chem. Soc.* **2004**, *126*, 3983−3995.

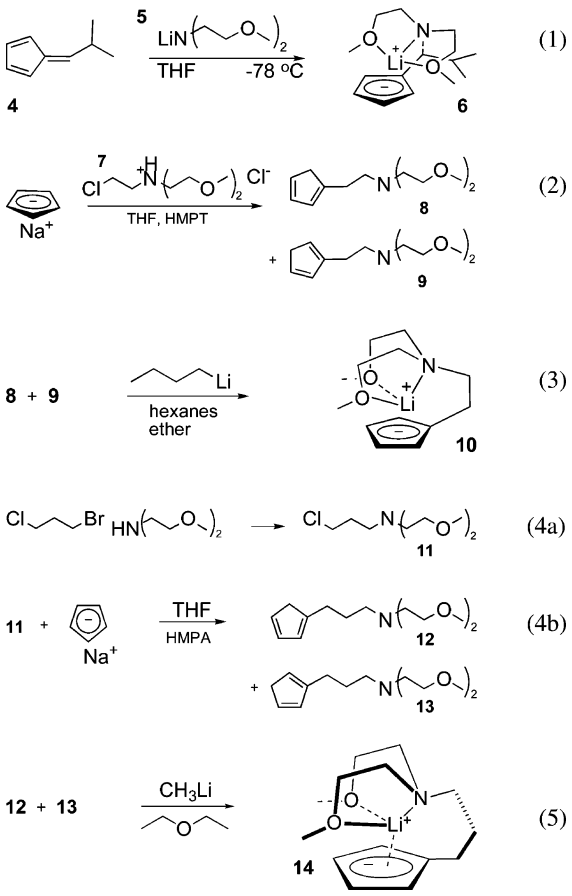

fulvene itself is unstable and inconvenient to prepare. NMR shifts of **6** in THF-d_8 solution are listed around the structure, in Table 1. Note that due to chirality at C_6 the isopropyl methyls are magnetically nonequivalent in the ^{13}C NMR as are also the NCH_2 carbons.

NOE $^7Li\{^1H\}$ HOESY[9] experiments confirm the proposed internally coordinated structure of **6**. Strong interactions are observed between ^7Li and protons on the ring, at ligand NCH_2 and one C-methyl, and much weaker interactions with protons at OCH_2 and OCH_3; see Figure 1.

At 170 K, ^{13}C NMR shows the ligand NCH_2 carbons of **6** to be nonequivalent due to the chirality at C_6 giving rise to an equal doublet. With increasing temperature, the latter progressively averages to a single sharp line by 230 K; see Figure 2. Line shape analysis gives rise to the activation parameters $\Delta H^{\ddagger} = 5.5 \pm 0.5$ kcal·mol^{-1} and $\Delta S^{\ddagger} = -16 \pm 1.5$ eu, Table 2.

Due to the fixed chirality at C_1 in **6**, the behavior described above can only be due to inversion at nitrogen. This requires decoordination of the pendant ligand to Li^+ prior to nitrogen inversion. Decoordination to the pendant ligand would most likely be accompanied by coordination of Li^+ to several THF molecules in the transition structure and the intermediates which might precede it. This would be consistent with the large negative $\Delta S^{\ddagger}$ value observed for nitrogen inversion.

We were unable to crystallize **6**; however, a model was constructed at the RHF[10,11] and B3LYP[11,12] levels of theory ultimately with basis set 6-311G* using starting structural parameters obtained from published crystallographic structures of other organolithium compounds.[7]

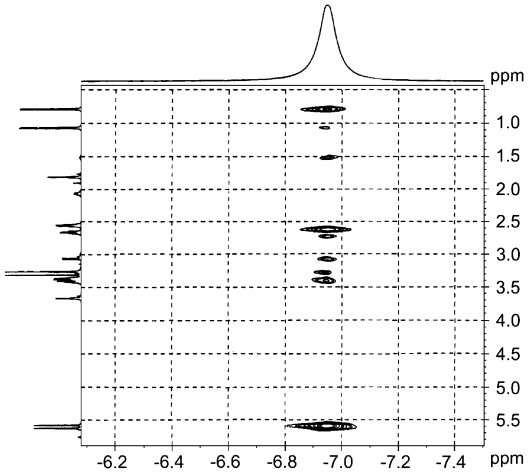

FIGURE 1. HOESY $^7Li\{^1H\}$ of **6**: mixing time 0.4 ms, in THF-d_8, 300 K. Resonances, MHz: ^1H, 300.1313; ^7Li, 116.641.

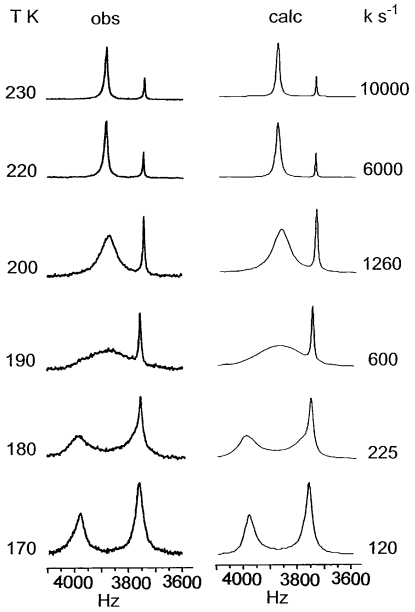

FIGURE 2. ^{13}C NMR line shapes, 6 NCH_2 part: left, observed at different temperatures; right, calculated with first-order rate constants. Line shape analysis takes account of the impurity resonance at 3750 Hz.

TABLE 2. Activation Parameters for Inversion Compounds 6 and 14

compd	^{13}C NMR used	$\Delta H^{\ddagger}$ (kcal·mol^{-1})	$\Delta S^{\ddagger}$ (eu)
6	NCH_2	5.5 ± 0.5	-16 ± 1.5
14	OCH_3	6.4 ± 0.5	-2.4 ± 0.3
14	NCH_2	5.6 ± 0.4	-8 ± 1

(8) (a) Qian, Y.; Li, G.; Chen, W.; Li, B.; Jig, X. *J. Organomet. Chem.* **1989**, *373*, 185. (b) Erker, G.; Nolte, R.; Krügar, C.; Schlund, R.; Bonn, R.; Grondey, H.; Mynott, R. *J. Organomet. Chem.* **1989**, *364*, 119. (c) Okuda, J. *Chem. Ber.* **1989**, *122*, 1075. (d) Howie, R. A.; McQuillan, G. P.; Thompson, D. W.; Lock, G. A. *J. Organomet. Chem.* **1986**, *303*, 213.

(9) (a) Reviewed: Bauer, W. NMR of Organolithium Compounds: General Aspects and Application of Two-Dimensional Heteronuclear Overhauser Effect Spectroscopy (HOESY). In *Lithium Chemistry, A Theoretical and Experimental Overview*; Sapse, A. M., Schleyer, P. v. R., Eds.; Wiley-Interscience: New York, 1995; pp 125−172. (b) Berger, S.; Miller, F. *Chem. Ber.* **1995**, *128*, 799−802.

Thus, in the current case the crystal structure of dimer **15**[7] was used to obtain the optimized structure of the monomer, **16**, confirmed to be a stable ground-state species with the usual frequency calculations. The latter was modified by replacing the terminal endo hydrogens with bonds to a HC═CH unit and then reoptimized to give **17**. Replacement of one C_6H hydrogen by isopropyl yields **6**. The resulting structural parameters are listed in Table 3. Carbon-13 shifts were then calculated for **6** using the B3LYP 6-311G* results in conjunction with GIAO.[13] Calculated shifts are quite close to the observed ones for most of the carbons; see Table 4. By contrast, using RHF 6-311G*/GIAO the calculated and observed shifts fitted badly. Each optimized structure was confirmed to be stable with the usual frequency calculations.[11]

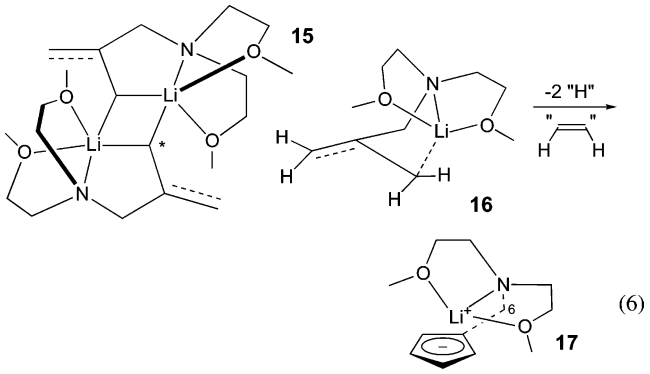

(6)

Compound **10** was prepared as shown in reactions 2 and 3. Carbon-13 and proton chemical shifts are listed around the structure in Table 1. Our crystals of **10** were not satisfactory for an X-ray crystallographic structure determination. However, we were able to construct a model by use of the buildup calculations similar to those described above to model **6**. Thus, insertion of a CH_2 into the ligand tether of previously optimized **17** followed by reoptimization provided a model for **10**.

$$\mathbf{17} \xrightarrow[\text{“}CH_2\text{”}]{} \mathbf{10}$$

TABLE 3. Structural Parameters B3LYP 6-311G* for Compounds 6, 10, and 14 and X-ray Crystallography Data for 14 (Bond Lengths (Å), Angles (deg))

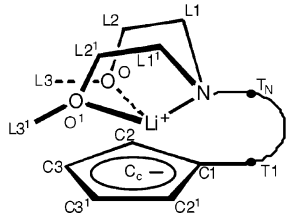

			14 X-ray cryst	14 B3LYP	10 B3LYP	6 B3LYP
C1	C2		1.4092 (17)	1.4172	1.4162	1.4238
C2	C3		1.4019 (17)	1.4154	1.4162	1.4115
C3	$C3^1$		1.3448 (18)	1.4143	1.4136	1.4143
$C3^1$	$C2^1$		1.4090 (18)	1.4167	1.4147	1.4102
$C2^1$	C1		1.4037 (17)	1.4176	1.4194	1.4222
Li	C1		2.306 (2)	2.2506	2.2233	2.1522
Li	C2		2.309 (2)	2.2659	2.2735	2.2852
Li	$C2^1$		2.313 (2)	2.2717	2.2843	2.2908
Li	C3		2.334 (2)	2.3026	2.3641	2.4851
LI	$C3^1$		2.332 (2)	2.3073	2.3719	2.4912
Li	C_C		1.9884 (18)	1.9354	1.9642	2.0120
Li	N		2.170 (2)	2.3021	2.3293	2.3625
Li	O		2.011 (2)	2.0997	2.1854	2.0712
Li	O^1		2.151 (2)	2.2221	2.0974	2.0959
N	L1		1.4714 (16)	1.4686	1.4705	1.4590
L1	L2		1.507 (2)	1.5261	1.5273	1.5311
L2	O		1.4222 (16)	1.4168	1.4259	1.4293
O	L3		1.4153 (16)	1.4180	1.4214	1.4218
N	$L1^1$		1.4728 (17)	1.4738	1.4685	1.4594
$L1^1$	$L2^1$		1.494 (2)	1.5191	1.5214	1.5287
$L2^1$	O^1		1.4172 (9)	1.4223	1.4256	1.4286
O^1	$L3^1$		1.4289 (18)	1.4213	1.4219	1.4219
C1	T1		1.4978 (18)	1.5054	1.5054	1.5173
T1	T2		1.5320 (19)	1.5430	1.5444 ($T1T_N$)	
T2	T_N		1.567 (2)	1.5354		
T_N	N		1.4976 (17)	1.4827	1.4754	1.5173
C_C	Li	N	125.19 (9)	127.4	113.38	100.06
C_C	Li	O	129.28 (10)	129.04	128.47	127.95
C_C	Li	O^1	125.51 (10)	126.99	129.30	128.32
N	Li	O	82.06 (7)	79.17	76.26	79.48
N	Li	O^1	81.69 (7)	78.40	80.59	79.12
O	Li	O^1	97.54 (8)	97.93	101.89	103.00
C_1	T_1	T_2	115.38 (11)	116.15	112.15	
T_1	T_2	T_N	115.70 (13)	115.69		
T_2	T_N	N	116.59 (12)	117.02	113.90	
C_1	T_N	N				109.23

TABLE 4. ^{13}C NMR Chemical Shifts (δ) for Compounds 6, 10, and 14, Calculated[a,b] and Observed[d] (for Numbering See Tables 1 and 3)

	6		10		14	
	calcd	obsd	calcd	obsd	calcd	obsd
C1	117.86	115.19	113.05	115.10	119.00	119.0
C2	103.53	102.18	104.55	101.6	101.64	102.0
C3	105.06	100.25	101.20	102.8	102.77	102.5
$C2^1$	105.42	102.18	99.28	102.6	101.67	102.0
$C3^1$	103.18	100.25	101.20	102.8	100.91	102.5
L1	53.65	49.26	58.39	51.8	49.21	54.1
L2	71.33	71.07	71.28	69.5	66.15	69.6
L3	54.63	56.37	54.28	58.6	53.70	58.5
$L1^1$	62.31	49.26	60.56	51.8	51.09	54.1
$L2^1$	70.51	71.07	69.30	69.5	66.64	69.6
$L3^1$	54.67	56.37	55.50	58.7	56.04	58.5
T1	67.22[c]	68.67[c]	29.81	28.7	31.68	32.6
T2			59.13[d]	56.4[d]	27.70	27.7
T_N	67.22[c]	68.67[c]	59.13[d]	56.4[d]	57.04	66.8

[a] B3LYP/6-311G*/GIAO. [b] δ scale. [c] T1 = T_N. [d] T_N = T2.

These results for optimized **10** were used to calculate[11] the ^{13}C chemical shifts using GIAO.[13] Whereas these shifts obtained from the HF 6-311G*[10] results are quite

(10) (a) Hartree, D. R. *Proc. Cambridge Philos. Soc.* **1928**, *24*, 89, 111. (b) Fock, V. *Z. Physik* **1930**, *61*, 126. (c) Reviewed, Parr, R. G.; Ellison, F. O. *Ann Rev. Phys. Chem.* **1955**, *6*, 171−192.

(11) Frisch, M. J.; Trucks, G. W.; Schlegel, H. B.; Scuseria, G. E.; Robb, M. A.; Cheeseman, J. R.; Zakrzewski, V. G.; Montgomery, J. A., Jr.; Stratmann, R. E.; Burant, J. C.; Dapprich, S.; Millam, J. M.; Daniels, A. D.; Kudin, K. N.; Strain, M. C.; Farkas, O.; Tomasi, J.; Barone, V.; Cossi, M.; Cammi, R.; Mennucci, B.; Pomelli, C. Adamo, C.; Clifford, S.: Ochterski, J.; Petersson, G. A.; Ayala, P. Y.; Cui, Q.; Morokuma, K.; Malick, D. K.; Rabuck, A. D.; Raghavachari, K.; Foresman, J. B.; Cioslowski, J.; Ortiz, J. V.; Stefanov, B. B.; Liu, G.; Liashenko, A.; Piskorz, P.; Komaromi, I.; Gomperts, R.; Martin, R. L.; Fox, D. J.; Keith, T.; Al-Laham, M. A.; Peng, C. Y.; Nanayakkara, A.; Gonzalez, C.; Challacombe, M.; Gill, P. M. W.; Johnson, B. G.; Chen, W.; Wong, M. W.; Andres, J. L.; Head-Gordon, M.; Replogle, E. S.; Pople, J. A. *Gaussian 98*, revision A.1; Gaussian, Inc.: Pittsburgh, PA, 1998.

(12) (a) Lee, C.; Parr, R. G. *Phys. Rev. B* **1988**, *37*, 785. (b) Becke, A. D. *Phys. Rev. A* **1988**, *38*, 3098. (c) Miehlich, B.; Savin, A.; Stoll, H.; Preuss, H. *Chem. Phys. Lett.* **1989**, *157*, 200. (d) Becke, A. D. *J. Chem. Phys.* **1992**, *96*, 2155.

(13) (a) Wolinski, K.; Hilton, J. F.; Pulay, P. *J. Am. Chem. Soc.* **1990**, *112*, 825. (b) Dodds, J. L.; McWeeny, R.; Sadlej, A. J. *Mol. Phys.* **1980**, *41*, 1419. (c) Ditchfield, R. *Mol. Phys.* **1974**, *27*, 789. (d) Cheeseman, J. R.; Frisch, M. J.; Trucks, G. W.; Keith, T. A. *J. Chem. Phys.* **1996**, *104*, 5497. (e) Keith, T. A.; Bader, R. F. W. *Chem. Phys. Lett.* **1992**, *194*, 1. (f) McWeeny, R. *Phys. Rev.* **1962**, *126*, 1028. (g) London, F. *J. Phys. Radium, Paris* **1937**, *8*, 397.

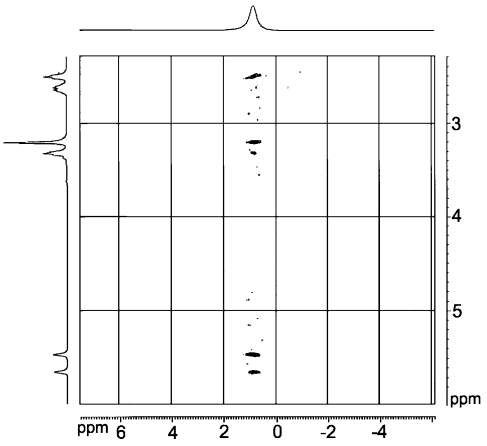

FIGURE 3. HOESY $^{7}Li\{^{1}H\}$ of **10**, in THF-d_8, 295 K.

TABLE 5. Ratios of Averaged Proton−Proton Separations from Proton Proton DPFGSE-NOE Experiments and B3LYP 6-311G* Calculations for Compound 10

	proton−proton separations			r_X/r_Y	
	irrad		obsd	NOE	B3LYP
X	OCH_3	to	C_3H, C_3, H	0.954	0.894
Y	OCH_3	to	C_2H, C_2, H		
X	OCH_2	to	C_3H, C_3, H	1.293	1.250
Y	OCH_2	to	C_2H, C_2, H		
X	NCH_2[a]	to	C_3H, C_3, H	1.270	1.247
Y	NCH_2[a]	to	C_2H, C_3, H		

[a] Ligand: NCH_2.

unsatisfactory, those from the B3LYP 6-311G*[12] procedure are remarkably close to the observed ones; see Table 2. We regard this agreement of calculated with observed ^{13}C chemical shifts as validating the B3LYP 6-311G* structure as a suitable model for **10**. This model is also consistent with the results of several NOE experiments. For example, a $^{7}Li\{^{1}H\}$ HOESY[9] experiment, Figure 3, shows interactions between ^{7}Li and all ring and ligand hydrogens, the strongest being to C_2H and $C_2'H$. The $^{7}Li-^{1}H$ interactions then decrease in the order to $OC\mathbf{H}_3$ and C_3H, $C_3'H$, the latter two together. Interactions with OCH_2 and NCH_2 protons are very weak.

In addition, an inverse HOESY $^{1}H\{^{7}Li\}$[14] buildup procedure gives the ratio of the ^{7}Li ring hydrogen distances shown in (7)

$$\frac{r^{7}\text{Li-C}_2\text{H, C}_{2'}\text{ H}}{r^{7}\text{Li-C}_3\text{H, C}_{3'}\text{ H}} = \frac{1.03\ (\text{NOE})}{1.048\ (\text{B3LYP})} \qquad (7)$$

close to the corresponding ratio of 1.048 from the B3LYP calculation.

In proton−proton DPFGSE-NOE build-up experiments, OCH_3, NCH_2, and OCH_2 proton resonances were separately irradiated and mixing times varied. Rates of C_2H, $C_2'H$, and C_3H, C_3'H proton resonance buildup, respectively, provide the ratios of average proton−proton separations; see Table 5. Comparison of the NOE-derived ratios with those from the B3LYP 6-311G*-optimized

(14) Alam, T. M.; Pedrotty, D. M.; Boyle, T. J. *Magn. Reson. Chem.* **2002**, *40*, 361−365. We thank Todd Alam for providing the pulse sequence and software.

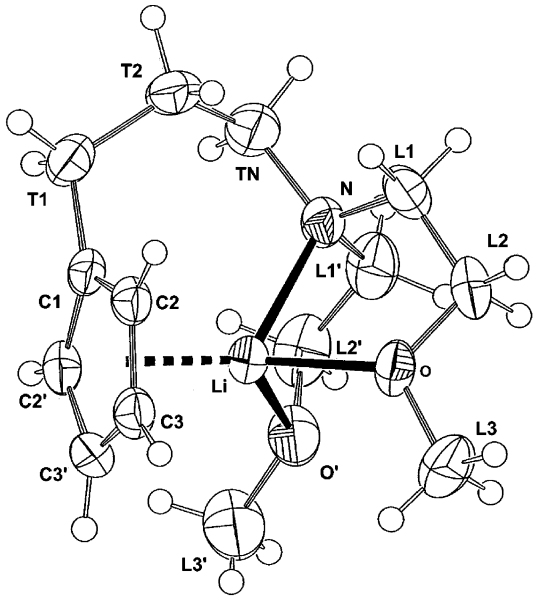

FIGURE 4. ORTEP diagram of **14** showing 50% thermal ellipsoids. Non-hydrogen atoms are labeled.

structure shows that the calculated structure is consistent with the NOE results.

X-ray crystallography of **14** reveals the internally solvated folded structure shown in Figure 4 and with selected parameters listed in Table 3. Each unit cell is occupied by two molecules related by a center of inversion. Carbon-13 shifts are listed in Table 1.

The X-ray structural parameters of **14**, Table 3, are all similar to results reported for a variety of externally solvated Cp^-Li^+ compounds[15] including a substituted triple ion, $(CpLiCp)^-$.[15e] All show similar Li^+ to Cp^- centroid distances within the range 1.9−2.0 Å.[15] These results all support a Cp^-Li^+ moiety whose structure is largely independent of the mode of lithium coordination. It appears that to accommodate the latter standard structure and internal coordination to Li^+ the C−C−C angles in the ligand tether of **14** widen relative to the tetrahedral angle while the H−C−H angles tend to close. For example, the angles for C−C−C and H−C−H around T2 are 115.69° and 105.35°, Table 3.

Prior to obtaining its crystal structure, a model for **14** was calculated using the building procedure described for compounds **6** and **10** above. Thus, a methylene was inserted into the optimized structure of **10** and the system was reoptimized first at the RHF[10,11] and then at the B3LYP[11,12] levels of theory, respectively, both using the 6-311G* basis set. The resulting structural parameters are listed in Table 3. Stabilities of all optimized structures were confirmed with frequency calculations. Using both sets of results, ^{13}C shift tensors were calculated using GIAO.[11,13] While the ^{13}C shifts obtained via RHF theory diverged significantly from the observed

(15) (a) Hammel, A.; Schwartz, W.; Weidlein, J. *Acta Crystallogr.* **1990**, *C46*, 2337−2339. (b) Lappert, M. F.; Singh, A.; Engelhard, L. M.; White, L. H. *J. Organomet. Chem.* **1984**, *262*, 271−278. (c) Jutzi, P.; Schlüter, E.; Kruger, C.; Pohl, S. *Angew. Chem., Int. Ed. Engl.* **1983**, *22*, 994. (d) Jutzi, P.; Schlüter, E.; Pohl, S.; Saak, W. *Chem. Ber.* **1985**, *118*, 1959−1967. (e) Gallucci, J. L.; Sivik, M. R.; Paquette, L. A.; Zaegel, F.; Mennier, P.; Gautherou, B. *Acta Crystallogr.* **1996**, *C52*, 1673−1679.

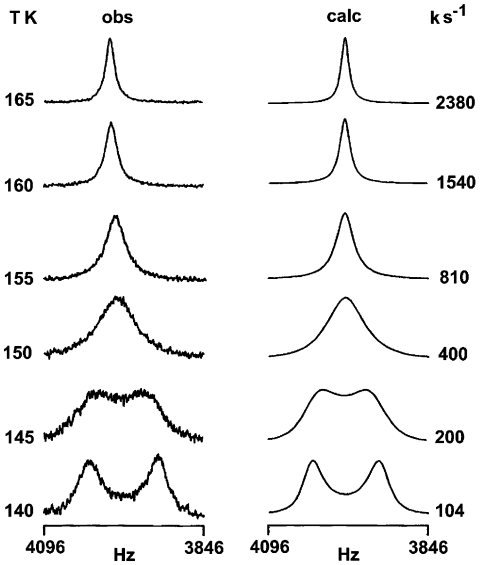

FIGURE 5. ^{13}C NMR, 75.476 MHz, line shapes, **14** in THF-d_8, ligand CH_2N part; left, observed at different temperatures; right, calculated with first-order rate constants.

ones, those from B3LYP optimization closely resemble the observed values; see Table 4. One can surmise that calculation of chemical shifts requires including electron correlation and exchange; both are incorporated at the B3LYP level of theory but not using RHF.

It is interesting that while most of the structural parameters for **14** from the X-ray crystallography and the B3LYP optimization are closely similar the stereochemistry around lithium is noticeably different; see Table 3.

In sum, we can regard the agreement of observed with calculated shifts as validating the B3LYP/6-311G*-optimized structure as a suitable model for **14** in nonpolar media.

The latter optimized structure is also qualitatively confirmed by the results of different NOE experiments. For example, a $^7Li\{^1H\}$ HOESY[9] experiment shows interactions of Li with all ring and ligand hydrogens. Also a proton proton DPFGSE-NOE[16] build-up experiment gave the ratio of averaged proton proton separations, see (8) where the subscripts indicate averaged distances[16] between methoxy protons and ring protons. The corresponding ratio from the above B3LYP structure is 0.85.

$$\frac{^{r}CH_3O\text{-}C_3H,\ C_3,\ H}{^{r}CH_3O\text{-}C_2H,\ C_2,\ H} = 0.92 \qquad (8)$$

The chirality of **14** is seen in the X-ray crystallographic data and is also evidenced by the magnetic nonequivalence of all ligand carbons in the solution ^{13}C NMR spectrum. Thus, at 140 K the CH_3O and CH_2N ligand ^{13}C resonances both consist of well-defined equal doublets. With increasing temperature above 140 K these two doublets progressively average to single lines at their respective centers, Figure 5. Line shape analysis[17] gives rise to the activation parameters listed in Table 2. These

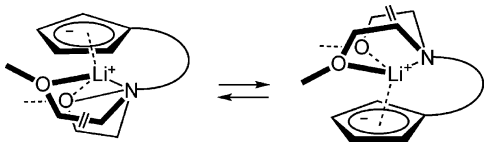

FIGURE 6. Inversion of **14** by face transfer.

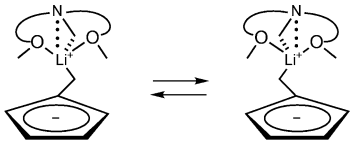

FIGURE 7. Inversion of **14** by lateral wobble.

values are considered to be sufficiently similar to reflect the same inversion process. Two mechanisms come to mind. They are transfer of coordinated Li^+ between faces of Cp^-, Figure 6, and inversion by lateral wobble, Figure 7. Face transfer of pendant ligand was proposed to account for inversion within internally solvated allylic lithium compounds.[7] Such a process for **14** would be expected to be accompanied by major changes in solvation, and thus, a large negative $\Delta S^{\ddagger}$ value would be expected. However, since the observed $\Delta S^{\ddagger}$ for inversion is almost neutral the lateral wobble mechanism, Figure 7, is more consistent with our data.

While CH_3Li is well-known to add to the exocyclic double bond of 6,6-dimethyl fulvene **18**[8a−d] under slightly different conditions (9), this same compound undergoes

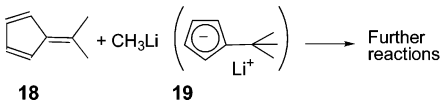

(9)

deprotonation, see for example (10).[18]

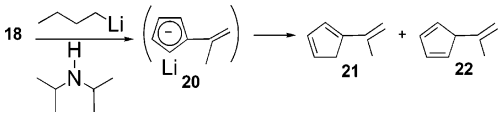

(10)

We have used equivalent reactions deprotonating fulvene **23** with a lithium amide, see (11), and with *n*-butyllithium (12) to form the 3-methylisopropenylcyclopentadienyllithium complexes **24** and **25**, respectively.

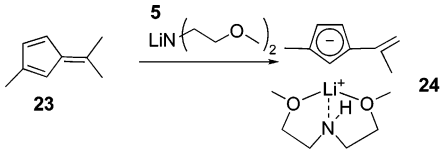

(11)

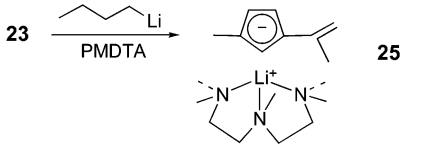

(12)

(16) (a) Bauer, W.; Sai, A.; Hirsch, A. *Magn. Reson. Chem.* **2000**, *38*, 500. (b) Bauer, W.; Gaul, C.; Arfidsson, P.; Seebach, D. NMR of Carbanions: Novel NOE Applications. *Sixth International Symposium on Carbanion Chemistry*, Marburg, Germany, July 20-Aug 1, 2001; Program Abstracts, p 94.

(17) (a) Kaplan, J. I.; Fraenkel, G. In *NMR in Chemically Exchanging Systems*; Academic Press: New York, 1980; Chapters 5 and 6. (b) Kaplan, J. I.; Fraenkel, G. *J. Am. Chem. Soc.* **1972**, *94*, 2907−2912. (c) Kaplan, J. I. *J. Chem. Phys.* **1958**, *29*, 462. (d) Alexander, S. S. *J. Chem. Phys.* **1962**, *37*, 967−974.

(18) (a) Nyström, J.-E.; Byström, E.; Ristoler, T.; Ekström, J. *Tetrahedron Lett.* **1988**, *29*, 4997. (b) Hoffmann, H. M. R.; Koch, O. *J. Org. Chem.* **1986**, *51*, 2939.

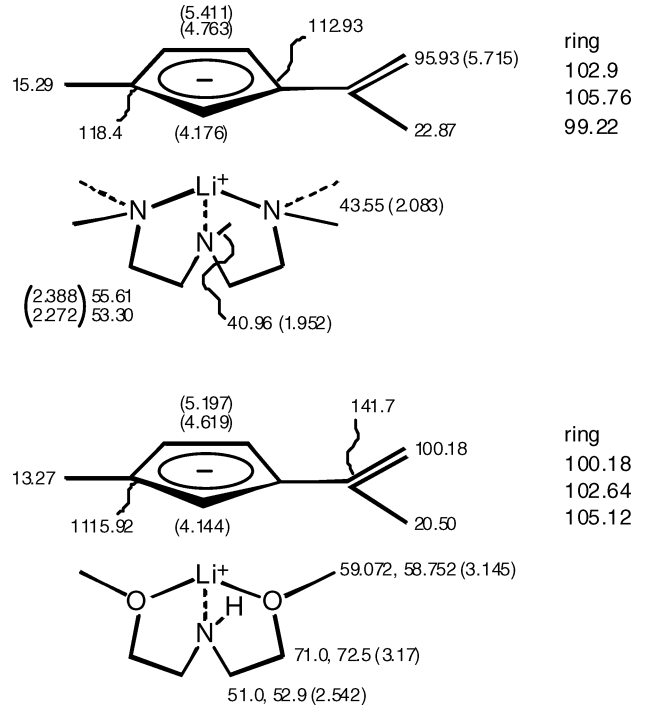

FIGURE 8. ^{13}C chemical shifts, δ scale, **24** and **25**, 295 K.

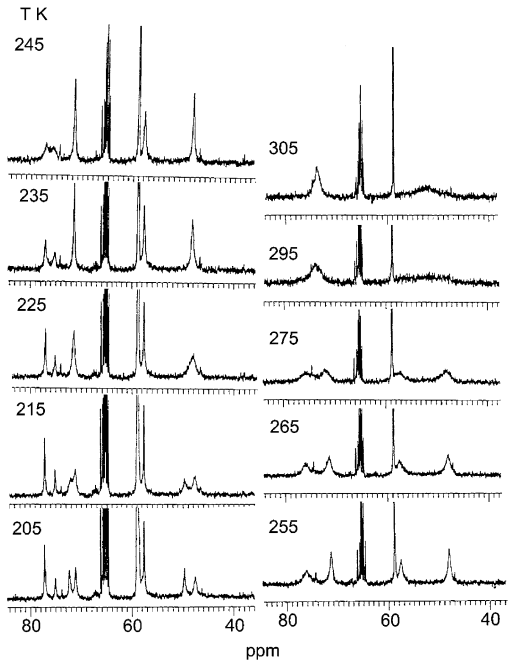

FIGURE 9. ^{13}C NMR **24** at different temperatures.

Chemical shifts are listed around the structures **24** and **25** in Figure 8.

At 205 K, ^{13}C NMR of **24** shows equal doublets centered at δ 48.5 and 71.5 due to, respectively, NCH_2 and OCH_2 while single lines at δ 77.12 and 57.19 are due, respectively, to OCH_2 and NCH_2 of unreacted amide; see Figure 9. Two closely spaced lines at δ 59.02 and 58.75 result from OCH_3 in both species.

Line shape changes observed in the ^{13}C NMR of the above sample are qualitatively indicative of two fast reorganization processes at equilibrium. Between 205 and 245 K the two ^{13}C doublets due to CH_2N and OCH_2 in the complex progressively average to single lines at their respective centers; see Figure 9, left side. This behavior is most likely due to inversion resulting from a combination of transfer of the coordinated ligand between faces of the carbanion and 180° rotation of ligand with respect to the anion.

Above 245 K, with increasing temperature a second dynamic process is evidenced by averaging of the ^{13}C resonances due to OCH_2 in **24** with OCH_2 in lithium amide **5** and in similar fashion the NCH_2 resonances of the two species also average. The overall process responsible for these changes necessarily involves a mutual exchange of the $(CH_3OCH_2CH_2)_2N^-$ moiety between free lithium amide **5** in solution with coordinated amine in **24**. It is not known whether mutual exchange of lithium takes place at the same time.

At room temperature, the ^{13}C NMR of the PMDT ligand of **25** consists of one single line each for the $N(CH_3)_2$ and NCH_3 methyls and two lines for the NCH_2's. On cooling this sample to 150 K the resonances due to $N(CH_3)_2$ and one NCH_2 broaden significantly. This behavior is qualitatively indicative of a fast equilibrium reorganization process within the ion pair whose rate increases with temperature.

General Remarks

Taken together, the crystallography of **14** and the NMR and calculational results for **6**, **10**, and **14** are all most reasonably consistent with monomeric internally coordinated structures for all three compounds. While the totality of the results support such structures the possible existence of higher aggregates cannot be eliminated. Models were built up of **6**, **10**, and **14** at the RHF[10,11] and B3LYP[11,12] levels of theory with basis set 6-311G* via a series of sequential optimizations and modifications starting with the crystallographic structure of an internally coordinated allylic lithium compound.[7] Each reoptimized structure was confirmed to be stable with the usual frequency calculation.

The RHF and B3LYP results in conjunction with the GIAO[13] procedure were used to calculate the ^{13}C NMR chemical shifts of **6**, **10**, and **14**. While shifts calculated from RHF theory agree poorly with the observed ones it is heartening that those from B3LYP/6-311G* are remarkably close; see Table 4. Clearly, at this point the confluence of theory with experiment validates B3LYP as providing suitable models for **6**, **10**, and **14**.

There are many common features among the X-ray crystallographic and calculational structural parameters of **6**, **10**, and **14**. The C−C, C−N, and C−O single bond lengths are typical of most organic molecules as are also the C−C−C, C−N−C, and C−O−C angles except for the C−C−C angles in the tethers. In addition, the Li Cp^- centroid distances in **6**, **10** and **14** both calculated and from the X-ray data for **14** are within the same 1.9−2.0 Å range as those reported in most structural studies of externally solvated Cp^-Li^+ compounds.[15] These include one which incorporates a triple ion $(CpLiCp)^-$ sandwich. Interesting also is the near coplanarity in **6**, **10**, and **14** of the sites C_c, Li, O, and O[1].

The structural features which vary significantly among **6**, **10**, and **14** are the angles and bond distances which

involve lithium including the distances Li−N and Li−O and the angles C_C-Li−N, Li−N−T_N, and to a lesser extent the angles N−Li−O, O−Li−O[1], and Li−N-L1. Note the large ca. 116° angles in the three-carbon ligand tether of **14** compared to 112° and 113.9° in the two-carbon tether of **10**. In addition, notice the not unexpected decrease of the Li−C_c−C_1 angle with decreasing length of the ligand tether.

That the Cp^-Li^+ moiety has a similar structure within so many solvated cyclopentadienyllithium compounds[15] including **6**, **10**, and **14** implies that this moiety has an inherent stability to which the rest of the ion-paired species accommodates. This is the reason for the variable C−C−C angles in the ligand tethers of **10** and **14** and in the variability of the bonding around lithium and nitrogen. Thus, a tether of variable length does not seriously perturb the Cp^-Li^+ interactions. The Cp^-Li^+ arrangement maintains its integrity. It is the tethers which are perturbed.

Experimental Section

NMR. Data were obtained using a deuterium-locked multinuclear spectrometer operating at frequencies of 300.1313, 75.476, and 116.641, all MHz, for, respectively, ^{1}H, ^{13}C, and ^{7}Li with provision for decoupling ^{7}Li from ^{13}C. Probe temperature was controlled and and calibrated by use of the secondary standards procedure.[19] NOESY, HOESY, and DPFGSE-NOE experiments were carried out following references given above. NMR line shape analyses were carried out as described previously.[17]

General Procedures. All manipulations of organolithium compounds, including crystallization of **14**, were conducted under an atmosphere of purified argon. Assigned structures of all compounds whose preparations are described below are consistent with their respective NMR data. Impurities, if present, were below the limits of NMR detection, except where noted.

1-Lithiocyclopentadienyl-1-bis(2-methoxyethyl)amino-2-methylpropane (6). To a solution of bis(2-methoxyethyl)-amine (400 mg, 3 mmol) in 3 mL of dry THF was added *n*-butyllithium (1.12 mL, 2.5 M, 2.8 mmol) in hexane at −78 °C. The reaction mixture was stirred at room temperature for 0.5 h. The resulting solution was then added to 6-isopropylfulvene,[20,21] **4** (360 mg, 3 mmol), dissolved in 3 mL of dry THF. The mixture was allowed to warm to room temperature and stirred for 2 h. ^{13}C NMR (THF-d_8, 62.9 MHz, 295 K) δ: 117.75, 104.59, 102.74, 73.70, 70.68, 58.77, 51.89, 32.10, 22.92, 22.34.

1-Isopropenyl-3-methylcyclopentadienyllithium·PMDTA Complex (25). A flamed-dried Schlenk tube was charged with a solution of 2,6,6-trimethylfulvene (240 mg, 2 mmol) and *N*,*N*,*N*′,*N*′,*N*″-pentamethyldiethylenetriamine (347 mg, 2.0 mmol) in 4 mL of dry diethyl ether. After the mixture was cooled to −78 °C, a solution of *tert*-butyllithium (1.6 mL, 1.2 M, 1.9 mmol) in pentane was added. The mixture was stirred at −78 °C for 2 h and then warmed to room temperature overnight. A 0.4 mL sample of the latter solution was used to prepare a 0.4 M solution of the organolithium compound in diethyl ether-d_{10}.

1-Isopropenyl-3-methylcyclopentadienyllithium·Bis-(2-methoxyethyl)amine complex (24). A flame-dried Schlenk tube was charged with bis(2-methoxyethyl)amine (2.79 g, 25 mmol) and 2 mL of diethyl ether. After the mixture was cooled to −78 °C, *n*-butyllithium (1.25 mL, 1.6 M, 2 mmol) was slowly added by syringe. The mixture was brought to room temperature and stirred for 30 min. After the mixture was cooled to −78 °C, 3,6,6-trimethylfulvene (2.4 g, 2 mmol) was added with stirring. After this addition, stirring was continued for 2 h at −78 °C and 1 h at room temperature. Solvent was removed under reduced pressure, and the residue was dissolved in 10 mL of diethyl ether. Of this solution, 1 mL was evaporated to dryness and the residue was dissolved to form a 0.4 M solution of the title compound in diethyl ether-d_{10} to be used for NMR study.

Acknowledgment. This research was generously supported by a grant from the National Science Foundation and in part by the M. S. Newman Chair of Chemistry. NMR equipment used was purchased with funds from NSF grants. We thank Dr. Charles Cottrell, Central Campus Instrumentation Center, for his untiring assistance and instruction in new NMR technologies.

Supporting Information Available: Crystallographic data, NMR data, Eyring plots, and *Z* matrixes. This material is available free of charge via the Internet at http://pubs.acs.org.

JO0512507

(19) (a) Duerst, R.; Merbach, A. *Rev. Sci. Intstrum.* **1965**, *36*, 1896. (b) Schneider, H. J.; Freitag, W.; Schoemmer, M. *J. Magn. Reson.* **1975**, *18*, 393. (c) Sikorski, W. H.; Sanders, A. W.; Reich, H. J. *Magn. Reson. Chem.* **1999**, *36*, 5118−5124.

(20) Stone, K. J.; Little, R. D. *J. Org. Chem.* **1984**, *49*, 1849−1853.
(21) Imafuku, K.; Arai, K. *Synthesis* **1989**, 501−505.